AD_____

Award Number: W81XWH-12-1-0138

TITLE: Early Detection of Amyloid Plaque in Alzheimer's Disease via X-Ray Phase CT

PRINCIPAL INVESTIGATOR: Xiangyang Tang

CONTRACTING ORGANIZATION: Emory University, Atlanta, GA 30322-1018,

REPORT DATE: June 2014

TYPE OF REPORT: Annual

PREPARED FOR: U.S. Army Medical Research and Materiel Command
Fort Detrick, Maryland 21702-5012

DISTRIBUTION STATEMENT: Approved for Public Release;
Distribution Unlimited

REPORT DOCUMENTATION PAGE

Form Approved
OMB No. 0704-0188

1. REPORT DATE	2. REPORT TYPE	3. DATES COVERED
June 2014	Annual	15 May 2013 - 14 May 2014

4. TITLE AND SUBTITLE

Early Detection of Amyloid Plaque in Alzheimer's Disease via X-Ray Phase CT

5a. CONTRACT NUMBER

5b. GRANT NUMBER
W81XWH-12-1-0138

5c. PROGRAM ELEMENT NUMBER

6. AUTHOR(S)

Xiangyang Tang

E-Mail: xiangyang.tang@emory.edu

5d. PROJECT NUMBER

5e. TASK NUMBER

5f. WORK UNIT NUMBER

7. PERFORMING ORGANIZATION NAME(S) AND ADDRESS(ES)

Emory University

Atlanta, GA 30322-1018

8. PERFORMING ORGANIZATION REPORT NUMBER

9. SPONSORING / MONITORING AGENCY NAME(S) AND ADDRESS(ES)
U.S. Army Medical Research and Materiel Command
Fort Detrick, Maryland 21702-5012

10. SPONSOR/MONITOR'S ACRONYM(S)

11. SPONSOR/MONITOR'S REPORT NUMBER(S)

12. DISTRIBUTION / AVAILABILITY STATEMENT
Approved for Public Release; Distribution Unlimited

13. SUPPLEMENTARY NOTES

14. ABSTRACT

In this project, we proposed to develop the imaging method for early detection of amyloid plaque in Alzheimer's disease. As specified in SA#1 and the project timeline, the major tasks of year 1 and year 2 are the construction and optimization of a prototype x-ray phase contrast CT system to carry out the tasks specified in SA#2 and #3. The prototype x-ray phase contrast CT has been built in the PI's Lab with preliminary performance optimization. The major challenge of the project is the fabrication of x-ray gratings at high precision and performance. Enabled by the cutting-edge opto-mechanical equipment and devices at the Nano-Technology Research Center of GaTech (see Fig. 1), we have fabricated the needed x-ray gratings through a trial-and-error process. We have evaluated the spatial resolution and low contrast detectability of the prototype x-ray phase contrast CT using specially designed phantoms. Thus far, under partial support of this award, two journal papers have been published in *Medical Physics* – one of the leading journals in medical imaging, and five papers published in leading international conferences. Overall, the project's progression has been in pace with the project timeline. Specifically, the prototype x-ray phase contrast CT is ready for carrying out the specimen study specified in statement of work (SOW).

15. SUBJECT TERMS
Alzheimer disease, Amyloid plaque, X-ray phase contrast, X-ray phase contrast imaging, X-ray phase contrast CT

16. SECURITY CLASSIFICATION OF:			17. LIMITATION OF ABSTRACT	18. NUMBER OF PAGES	19a. NAME OF RESPONSIBLE PERSON
c. REPORT	b. ABSTRACT	c. THIS PAGE			USAMRMC
U	U	U	UU	15	19b. TELEPHONE NUMBER *(include area code)*

Table of Contents

Introduction

A. Overall: As the elderly population increases, dementia due to Alzheimer's disease (AD) has emerged as a major threat to human health[1-3]. Recently, the x-ray CT based on a new imaging mechanism – refraction – is emerging as a new technology to improve CT's capability of differentiating soft tissues[4-10]. Hence, we propose to develop the x-ray phase contrast CT imaging method with an x-ray tube and gratings for direct detecting of amyloid plaques in Alzheimer's brain. It is hypothesized that the disparity in refractive property can generate contrast between the amyloid plaques and surrounding neuronal tissues in AD and the contrast is sufficient for imaging. Without the involvement of contrast agent or molecular probes, the so-called BBB (brain blood barrier) can thus be avoided. The project started on 05/15/2012. Here is the annual report of the project's progress in year 2. In order to be objective and complete, some of the important progresses made in year 1 may be mentioned as well, while this report is focusing on the major progress made in year 2.

B. Specific Aims:

Three Specific Aims specified in the proposal's Statement of Work (SOW), which are repeated below:

SA#1 Develop and optimize an x-ray phase CT to explore the methodology of direct imaging of AP;
Outcome: An x-ray tube- and grating-based phase CT as the foundation for the pursuit of SA #2 and #3.

SA#2 Evaluate the x-ray phase CT's capability of imaging $A\beta_{1\text{-}40}$/$A\beta_{1\text{-}42}$ peptides/fibrils at the concentrations existing in AD brain;
Outcome: A quantitative understanding of x-ray phase CT's capability in imaging the $A\beta_{1\text{-}40}$ and $A\beta_{1\text{-}42}$ fibrils.

SA#3 Verify the x-ray phase CT's capability of direct imaging of AP in AD using postmortem brain specimens.
Outcome: Quantitatively evaluated and verified performance of x-ray phase CT for imaging APs in AD.

C. Project Timeline:

The project timeline specified in the project's SOW is also listed below:

Tasks	Q1	Q2	Q3	Q4	Q5	Q6	Q7	Q8	Q9	Q10	Q11	Q12
D.1.1: System construction												
D.1.2: System optimization												
D.2: Performance: Phantom study												
D.3: Performance: Specimen study												

Body

According to the project timeline, the major tasks in the second year are System Optimization and preliminary Phantom Studies. The prototype x-ray phase contrast CT built in the PI's lab for carrying out this project consists of a micro-focus tube, a CMOS flat panel x-ray detector with 48μm detector cell dimension, and the two key components – x-ray gratings G1 and G2. The imaging performance of this prototype system has gone through a preliminary system optimization, with an emphasis to improve the performance of G1 and G2. At the time of this annual report is being prepared, this prototype x-ray phase contrast CT system is working in the PI's Lab at its full functionality as anticipated (see Fig. 1), although its performance may be further improved by continuous effort in grating fabrication and system optimization. Below is a summary of

the major progresses made in year 2, including the progress in key Subsystem/Components, System Integration and Optimization, System Performance, and preliminary results of Phantom Study.

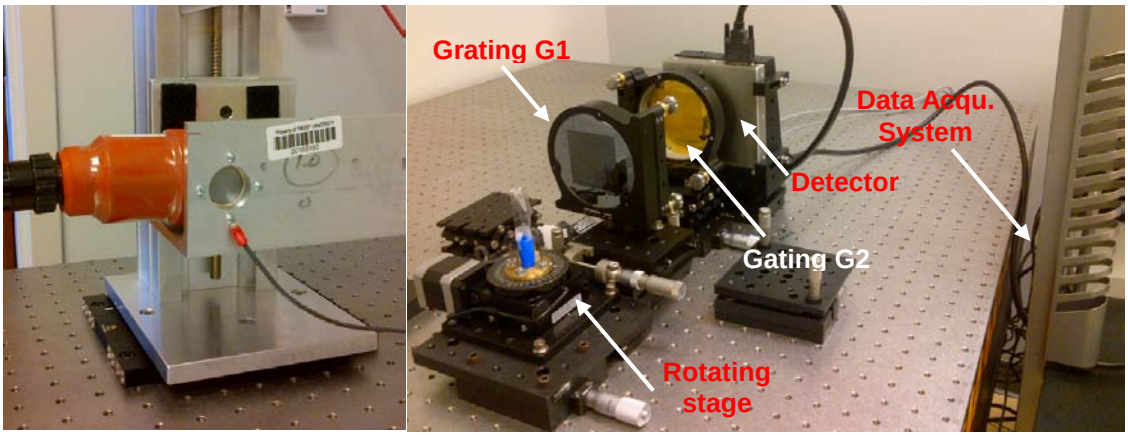

Figure 1. A picture showing the prototype x-ray phase CT system: (a) the micro focus x-ray tube and (b) the rest of the system.

A. **Subsystem/components – Grating G1 and G2**: The fabrication of grating G1 and G2 is very challenging, since the wavelength of x-ray is very short (~0.1 – 0.01*nm*). Using the cutting-edge opto-mechanical, chemical and physical equipment and devices at the GaTech's Nano-Technology Research Center (NTRC) (see Fig. 2), a set of x-ray gratings G1 and G2 for building the prototype x-ray phase contrast CT have been successfully fabricated (see Fig. 3). It turns out that the fabrication of the gratings, especially grating G2, is significantly more challenging than expected. With substantial dedicated effort and going through an extensive error-and-trial process, the performance of the gratings G1 and G2 that have been integrated into the prototype system is relatively satisfactory, even though further effort is being invested to obtain more gratings G1 and G2 with even higher quality.

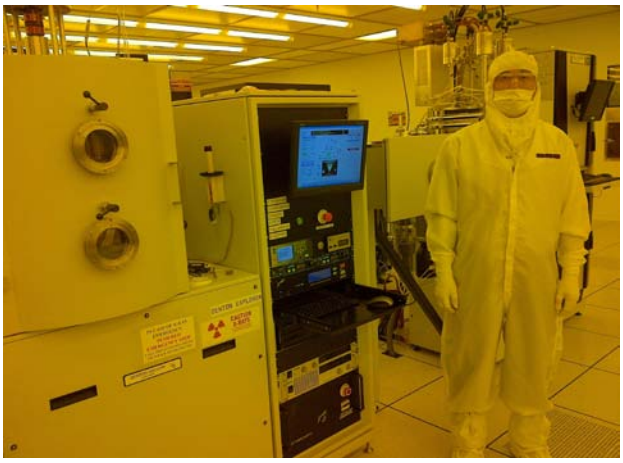

Figure 2. A picture showing that the PI is in the clean room of GaTech's Nano-Technology Research Center, standing by the Denton Explorer E-beam evaporator for the fabrication of grating G2, a key component of the prototype x-ray phase contrast CT system.

Shown in Fig. 3 (a) and (b) are the microscopic pictures of gratings G1 and G2. The periods of G1 and G2 are 8 and 4.6 μm, respectively, and thus their micro-structure are not visible to naked eyes. Presented in Fig. 3 (c) is a picture showing the installation of gratings G1 and G2 in the prototype x-ray phase contrast CT system. As illustrated, the gratings G1 and G2 are installed in Low Wave-front Distortion mirror mounts made by Newport Corporation. To make an almost-perfect mechanical alignment among the gratings and x-ray detector, each grating is mounted on a solid platform with three-axis tilting capability.

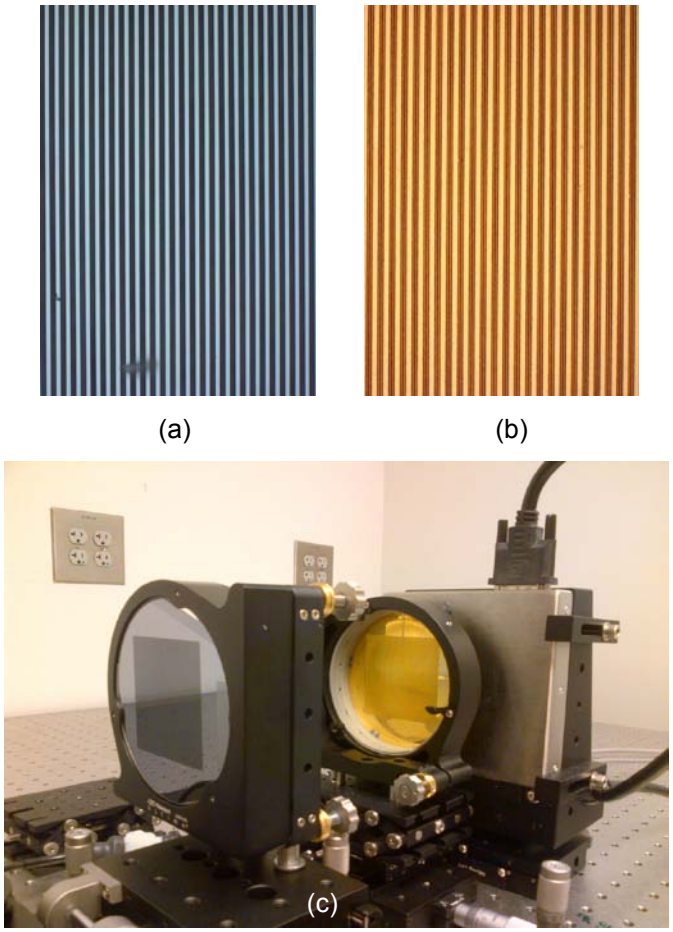

Figure 3. The microscopic pictures of grating G1 (a) and G2 (b) and a picture showing how they are installed in the prototype x-ray phase contrast CT system (c).

B. **Subsystem/components – Aβ-peptide phantoms**: As specified in SA#2 of the SOW, using the specially designed Aβ-phantoms, we'll investigate the contrast-to-noise ratio (CNR) of $A\beta_{1\text{-}40}$ and $A\beta_{1\text{-}42}$ fibrils in the x-ray phase contrast CT imaging, as a function over the molar concentrations corresponding to normal, pathologic and Alzheimer's brains, in which the amyloid precursor protein (APP) will be included as a reference. Toward this goal, we have made three PMMA (Polymethyl methacrylate) frames for installing the Aβ-phantoms, and shown in Fig. 4 (a) are the major parts (bodies and caps). As initially specified, the tunnels drilled in the PMMA body will be filled with $A\beta_{1\text{-}40}$/$A\beta_{1\text{-}42}$ peptides/fibrils solutions at selected concentrations (see Table I). The Aβ-phantoms with the $A\beta_{1\text{-}40}$ and $A\beta_{1\text{-}42}$ fibrils

filled and sealed will be installed in the rotation stage of the prototype x-ray phase contrast CT in the way illustrated in Fig. 1 (b) to carry out the tasks toward SA#2. However, to avoid biological decay, these targets filled with the $A\beta_{1\text{-}40}$ and $A\beta_{1\text{-}42}$ and their fibrils have to be stored in refrigerator at -20 C°. In order to be convenient for storage and repeated scan, the $A\beta_{1\text{-}40}$ and $A\beta_{1\text{-}42}$ peptides and fibrils are filled in PCR (Polymerase Chain Reaction) tubes as illustrated in Fig. 4 (b). These Aβ targets are stored in refrigerator and are mounted on the top of the Aβ-phantom (Fig. 4 (a)) during scan and data acquisition.

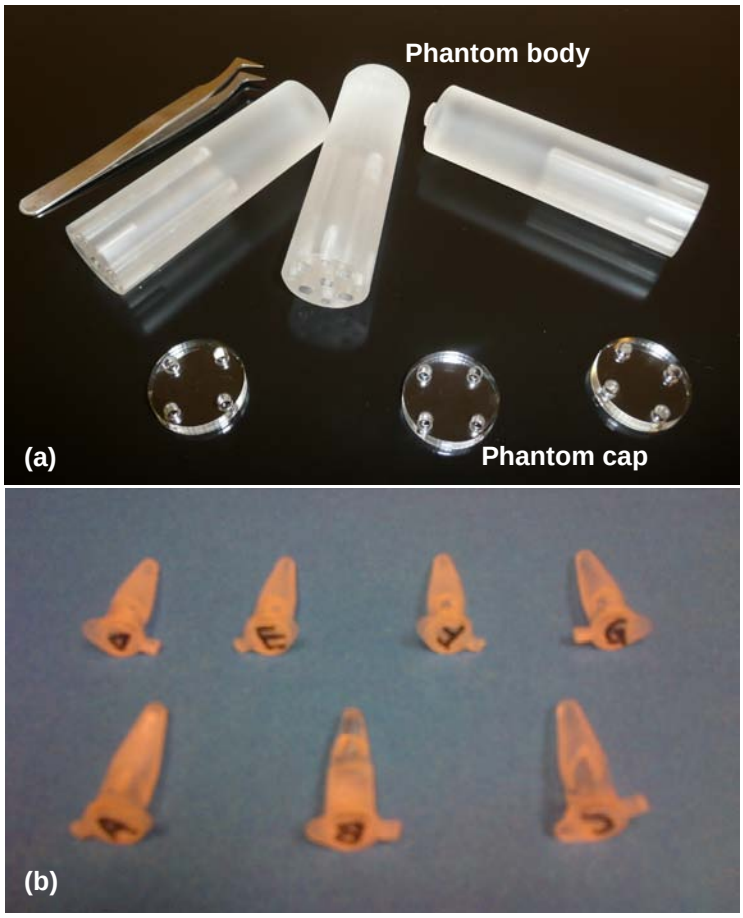

Figure 4. A picture showing: (a) the phantom body made of PMMA for making the image quality phantom and (b) the PCR tubes filled with amyloid precursor protein (A) and Aβ peptides (B, C, D) and Aβ peptides/fibrils (E, F, G) to be installed on top of the phantom body (see Table I).

Table 1. Phantom configuration and Aβ-peptide concentration[10] (Unit of molar concentration: pm/g).

Phantoms	I	II	III	IV
Image quality	H_2O	POM: $(CH_2O)_n$	PTFE: $(C_2F_4)_n$	LDPE: $(C_2H_4)_n$
Aβ-Peptide (pmol/g)	APP (2/2)	$A\beta_{1\text{-}40}/A\beta_{1\text{-}42}$ (2/2) [B]	$A\beta_{1\text{-}40}/A\beta_{1\text{-}42}$ (33/1117) [C]	$A\beta_{1\text{-}40}/A\beta_{1\text{-}42}$ (661/2100) [D]
Aβ-Peptide:Aβ-fibril (pmol/g)	APP (2/2)	$A\beta_{1\text{-}40}/A\beta_{1\text{-}42}$-Peptide: $A\beta_{1\text{-}40}/A\beta_{1\text{-}42}$ -Fibril (0.5/0.5:0.3/1) [E]	$A\beta_{1\text{-}40}/A\beta_{1\text{-}42}$-Peptide: $A\beta_{1\text{-}40}/A\beta_{1\text{-}42}$-Fibril (1.6/9:19/1172) [F]	$A\beta_{1\text{-}40}/A\beta_{1\text{-}42}$-Peptide: $A\beta_{1\text{-}40}/A\beta_{1\text{-}42}$-Fibril [G](4.4/11.1:159/1659)

C. **System integration:** The prototype x-ray phase contrast CT has been developed in the PI's laboratory (see Fig. 1), with preliminary system performance optimization (see section D below). Except for the data acquisition system and the computer that controls the operation and synchronization of stage rotation, data transferring, data correction and image reconstruction, all subsystems and components are installed on the top of a high-end optical table made by Newport Corporation and located in a room of the PI's lab with x-ray shielding.

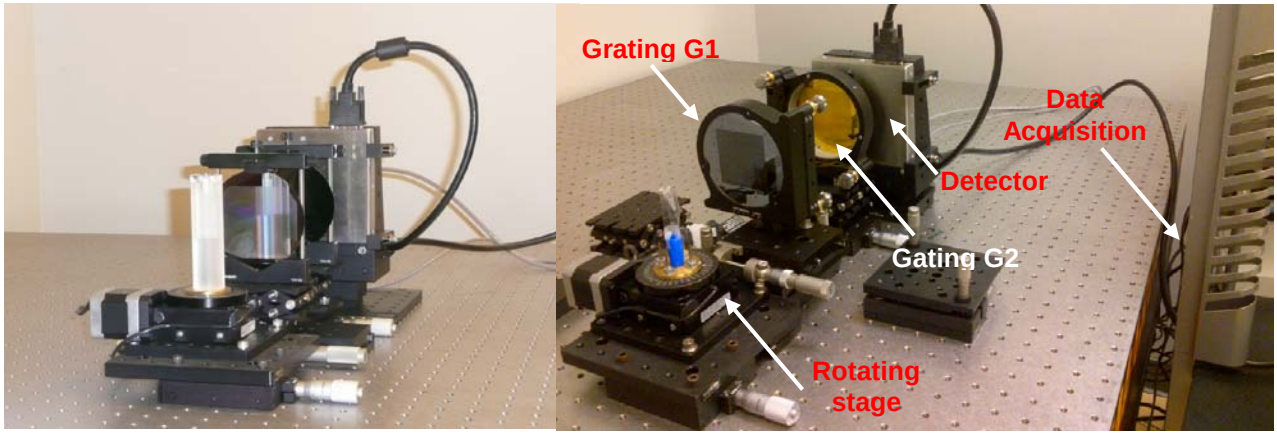

(a) **(b)**

Figure 5. Pictures showing the prototype x-ray phase contrast CT: (a) configuration of the initial x-ray phase contrast CT system and (b) the prototype system with performance initially optimized.

D. **System optimization**: The most challenging task in this project is the fabrication of high accuracy and precision x-ray gratings. The second most challenging task is the installation and alignment of gratings G1 and G2. As illustrated in Fig. 5, initially, gratings G1 and G2 are mounted in the so-called vertically locked holders (VLH, made by Newport Corporation) that are installed on the linear movable stages. It has been found that the radial force applied by the VLH may distort the shape of gratings G1 and G2 that are made of 4 inch silicon wafers and thus degrades their optical property significantly. To address this issue, two high-end low wave-front distortion mirror holders are employed to mount the gratings. It also has been found that, to have an acceptable alignment among gratings G1 and G2 and the flat panel x-ray detector, their orientation needs to be adjusted as well. Hence, each grating is mounted on a stage that can rotate respectively along the x, y and z axis, respectively. The detail of mounting and alignment of gratings has been pictured in Fig. 3. As shown in Fig. 5 (a) and (b), with a mechanical optimization, the prototype x-ray phase contrast CT system (Fig. 5 (b)) becomes much more complicated than the initial implementation (Fig. 5 (a)).

Another major challenge in an x-ray CT system integration is that any imperfection in the x-ray detector's performance, even though its magnitude is only 0.1% relatively to what is supposed to be, may result in severe ring artifacts[11]. Illustrated in Fig. 6 (a) is an example of the images obtained using the attenuation-based imaging chain of the prototype x-ray phase contrast CT system built in the PI's Lab, wherein ring artifacts exist. The image reconstruction algorithm in reference[12] was utilized to reconstruct the CT images. As demonstrated in Fig. 6 (b), with a specially designed post-image-formation algorithm, the ring artifacts were removed completely. Since this ring removal algorithm is post-image-formation, it is applicable in not only the attenuation based conventional CT but also the x-ray phase contrast CT.

In addition, we have developed the pre-reconstruction algorithms to remove the beam-hardening artifacts that can exist in the images of not only the conventional attenuation-based CT but also the phase contrast CT. Demonstrated in Fig. 6 (c) is an example to show the efficacy of such pre-reconstruction algorithms.

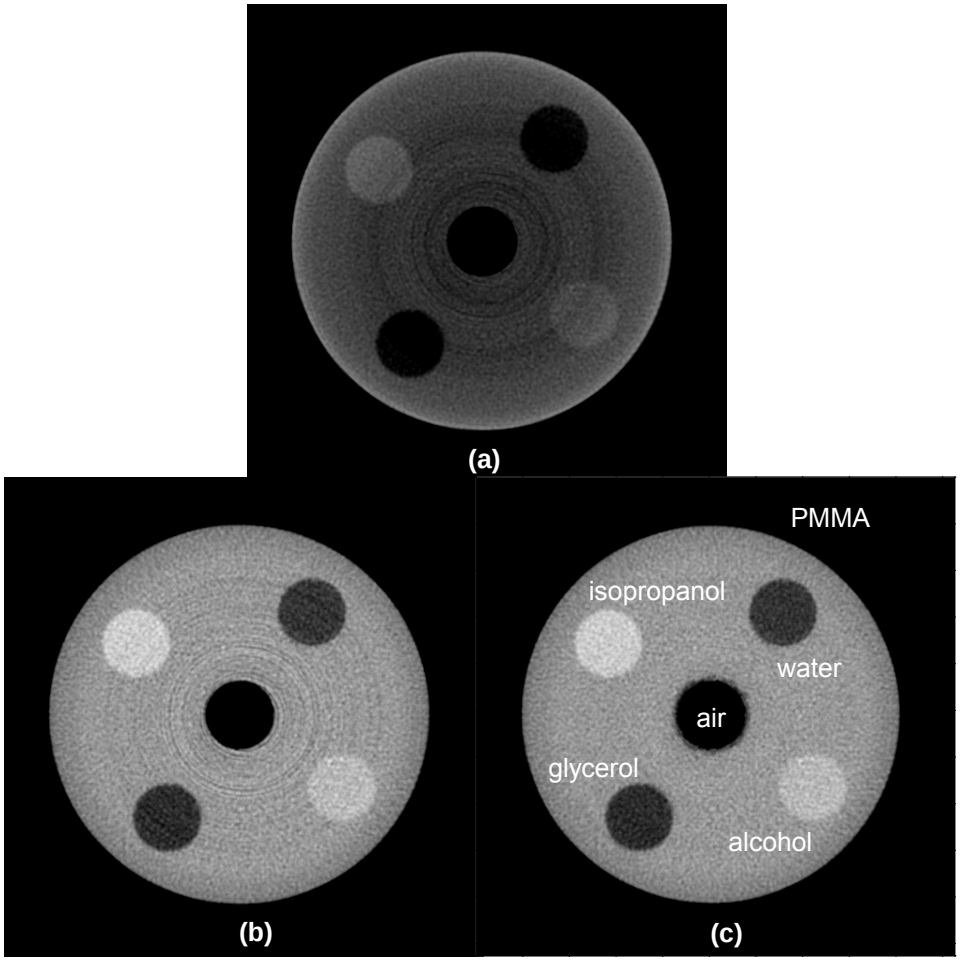

Figure 6. The conventional CT images of the IQ phantom with: (a) Beam-hardening and spectral artifacts, (b) Beam-hardening artifacts eliminated, and (c) Both beam-hardening and spectral artifacts removed.

E. **Preliminary System performance**: In general, the imaging performance of a CT system is assessed by its low contrast detectability, spatial resolution and temporal resolution. As specified in the SOW, the goal of this research project is to develop the x-ray phase contrast CT imaging method for early detection of amyloid plaque in Alzheimer's disease. Because the amyloid plaques are small in size and low in contrast against the surrounding tissues, the x-ray phase contrast CT imaging of amyloid plaques requires superior spatial resolution and low contrast detectability simultaneously.

a. **Spatial Resolution**: As indicated and experimentally evaluated in reference[8,13], the spatial resolution of an x-ray phase contrast CT is virtual identical to that of its attenuation-based counterpart, i.e., the conventional CT (namely virtual equivalence of spatial resolution). The figure of merit (FOM) to assess the spatial resolution of a conventional CT system is the MTF (modulation transfer function). The methods for gauging the MTF of a conventional CT system have been well established in the literature[14], in which a high contrast thin object, such as a thin metal wire, is usually employed. In principle, the wire should be thinner than the x-ray detector cell's dimension. However, the detector cell dimension of the prototype x-ray phase contrast CT in our investigation is $48\mu m$. Note that, a wire that is thinner than $48\mu m$ may not be able to withstand the force exerted on it to keep it straight and parallel to the CT's axis

of rotation during the projection data acquisition process. Hence, alternatively, using a wire of approximately 100μm diameter, we measure the MTF of the CT system with two detector cells binned together and the result attained is presented in Fig. 7. In such a way, the MTF of the conventional counterpart of the x-ray phase contrast CT without the 2× detector cell binning, i.e., at the default 48μm detector cell dimension, can be approximately obtained through proportional projection. Moreover, due to the virtual equivalence in the spatial resolution[8,13] between the x-ray phase contrast CT and the conventional CT, we can indirectly obtain the MTF of the prototype x-ray phase contrast CT.

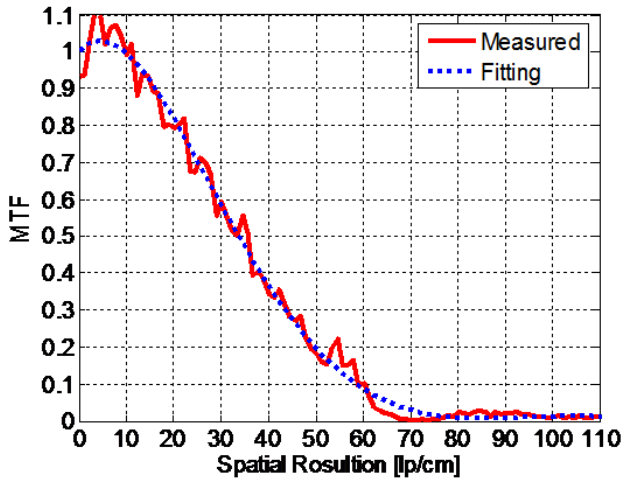

Figure 7. The MTF corresponding to the attenuation-based counterpart of the x-ray phase contrast CT with 2 detector cells binned together, which can be used to estimate the projected MTF corresponding to the x-ray phase CT without detector cell binning.

b. Low Contrast Detectability: With the prototype x-ray phase contrast CT system available in the PI's lab, two specially designed phantoms are utilized to gauge the low contrast detectability. The first is a phantom made of a gold fish, and the images corresponding to the contrasts generated by attenuation, differential phase and dark-field are presented in Fig. 8 (a) – (c), respectively. It is clearly demonstrated that both the differential phase contrast and dark-field contrast are indeed different from the attenuation contrast, especially at the interface between soft tissues and low attenuation material, e.g., the soft-tissue/air-bladder and soft-tissue/bone interfaces. It is observed that the vast majority of the structures rendered by the differential phase and dark field contrasts are not visible in the images corresponding to the attenuation contrast. Hence, it should be fair to say at this stage that the differential phase and dark-field contrasts are at least complementary to the attenuation contrast and thus may improve x-ray CT's capability in differentiating soft tissues.

The second phantom is made of water, air and cotton, which are installed in a PCR tube. The bottom segment of the PCR tube is filled with water and its top segment is inserted with a piece of cotton, whereas its mid-segment is left alone, i.e., filled with air. As anticipated, the water generates contrast in the image corresponding to the attenuation contrast, as illustrated in Fig. 9 (a). Meanwhile, cotton is of very low attenuation and thus should generate little contrast in the attenuation-based images, as confirmed in Fig. 9 (a). However, we do observe very strong contrasts generated by cotton in the images (Fig. 9 (b) and (c)) corresponding to the differential phase contrast and dark-field contrast, respectively. This clearly shows us that certain material that is of little attenuation and generate almost no contrast in the attenuation-based image can generate very strong contrast in the differential phase contrast and dark-field based images. It is believe that the underlying reason for cotton to generate the strong differential phase contrast and dark-field contrast is its fine fabric structure. It should be noted here that

the $A\beta_{40\text{-}42}$ peptides, especially those fibriled $A\beta_{40\text{-}42}$ peptides, is also of fine structures and thus may generate contrast in differential phase contrast and dark-field contrast images.

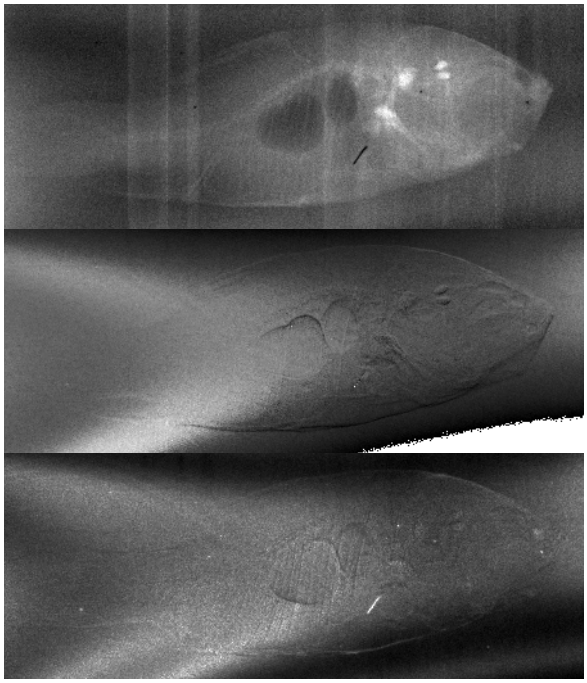

Figure 8. The projection (radiographic) images of a gold fish corresponding to: (a) attenuation contrast, (b) differential phase contrast, and (c) dark field contrast (detector cell: 96 μm).

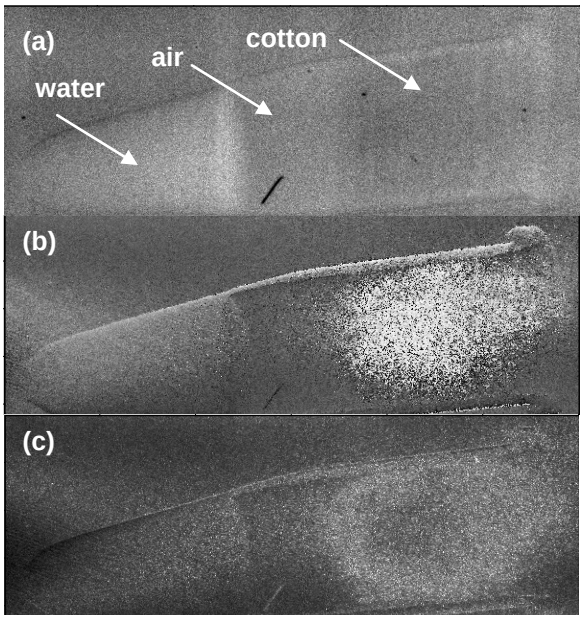

Figure 9. The projection (radiographic) images of a phantom made of cotton and water: (a) attenuation contrast, (b) differential phase contrast, and (c) dark field contrast (detector cell: 48 μm).

F. **Preliminary Phantom Study**: As listed in Table I, seven Aβ peptide targets are to be studied before the investigation with AD brain specimens. Presented in Fig. 10–12 are images of the Amyloid Precursor

Protein (APP), $A\beta_{1-40}/A\beta_{1-42}$ (2/2), and $A\beta_{1-40}/A\beta_{1-42}$ (33/1117), respectively, corresponding to the attenuation, differentia phase and dark-field contrasts, sequentially. Due to space limitation, the images of other targets are not presented. The phase contrast images of these Aβ targets are being analyzed. Meanwhile, the projection data of these targets for phase contrast CT imaging have been acquired and are being pre-processed for image reconstruction using the algorithm published in reference[12].

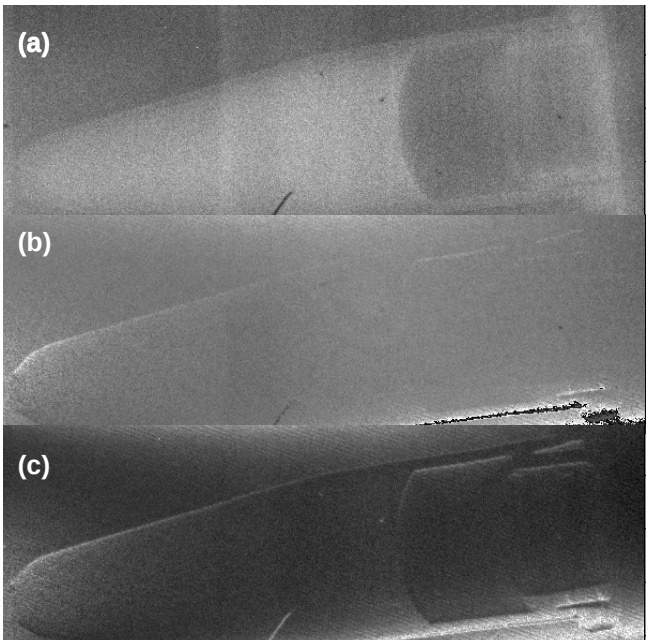

Figure 10. The projection (radiographic) images of the APP target in the Aβ-phantom: (a) attenuation contrast, (b) differential phase contrast, and (c) dark field contrast (detector cell: 48 μm).

Major Accomplishments in Year 2

- **System Integration and Performance Optimization:** The prototype x-ray phase contrast CT has been built and working at its full functionality as a "three-in-one" imaging system that generates images corresponding to the attenuation, differential phase and dark field contrast, respectively. The imaging performance of the prototype system has been optimized by significantly improving the quality of the key components – gratings G1 and G2, as well as the mechanical accuracy and precision in optical component installation and alignment.

- **Preliminary Phantom Study:**
  - Radiographic images of the Aβ-phantom have been acquired and analyzed. Based on image quality analysis, the methods to correct for background non-uniformity and phase wrapping have been designed and implemented.
  - Projection data of the Aβ-phantom for generating x-ray phase contrast tomographic images have been acquired, which will be processed and reconstructed in three contrasts – attenuation, refraction and dark field, respectively, in the up-coming months.

- **Investigation of the Dark Field Contrast as a Complex Signal**: It has been an existing understanding that the signal corresponding to the dark-field contrast is real. Based on an in-depth theoretical derivation, analysis and computer simulation, we have discovered that the signal of dark field contrast is actually complex and manifests its imaginary part while the fine structure of an object to be imaged is

smaller than the dimension of the detector cells used for data acquisition. We have derived the analytic formulae to describe the existence of the imaginary part of the complex dark field contrast signal. An approach to retrieve the imaginary part for imaging has also been proposed. The theoretical and simulation results have been put into a manuscript and submitted to Medical Physics for publication[15].

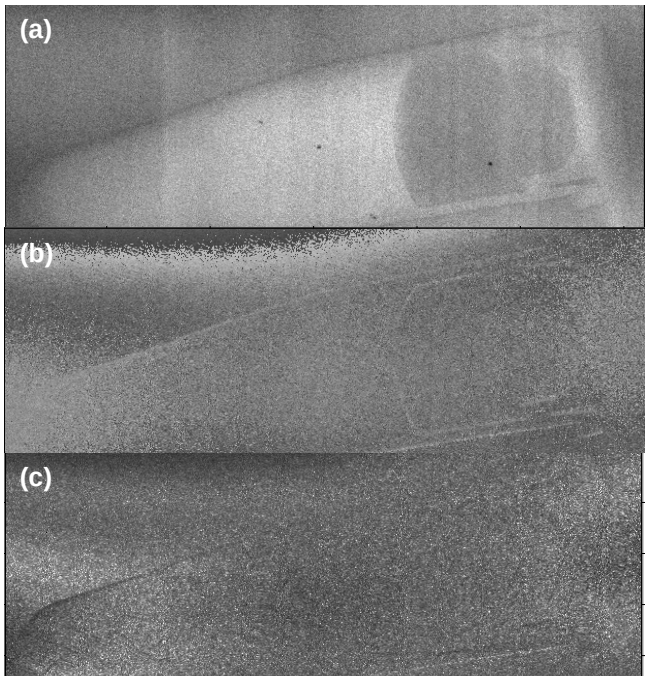

Figure 11. The projection (radiographic) images of the APP-B target in the Aβ-phantom: (a) attenuation contrast, (b) differential phase contrast, and (c) dark field contrast (detector cell: 48 μm).

Reportable Outcomes: In Year 2, one paper related to the project have been submitted to Medical Physics, one of the leading scientific journals in medical Imaging, for possible publication. In addition, 3 papers have been published in international conferences, such as the SPIE Medical Imaging Conference, AAPM (American Association of Physicist in Medicine) and RSNA (Radiological Society of North America). In addition, it is worthwhile mentioning that one team member (a post-doc fellow) has finished his training as a post-doc fellow that is partially supported by this award and found a faculty position.

A. Publication in Peer-reviewed Journals

1. Yang Y and Tang X, "Complex dark-field contrast and its retrieval in x-ray phase contrast imaging implemented with Talbot interferometry," submitted to *Med. Phys.*, in review.

B. Publication in Peer-reviewed Conferences

1. X. Tang and Y. Yang, "Bipolar contrasts generated by microbubbles in grating-based x-ray phase contrast CT," RSNA (Radiological Society of North America) 99th Scientific Assembly and Annual Meeting, *Chicago*, USA, Dec. 1 – Dec. 6, 2013. (Oral presentation)
2. X. Tang, Y. Yang and S. Tang, "Detectability index and its variation in differential phase contrast CT compared with the conventional CT – A channelized Hottelling observer study,"

55th Annual Meeting of AAPM (American Association of Physicist in Medicine, *Indianapolis*, *IN*, August 4-8, 2013. (Oral presentation)

3. X. Tang, Y. Yang and S. Tang, "Detectability index of differential phase contrast CT compared with conventional CT: A preliminary channelized Hotelling observer study," *SPIE Proc.* vol. 8668, doi: 10.1117/12.2008015, 866854, 10 pages, 2013.

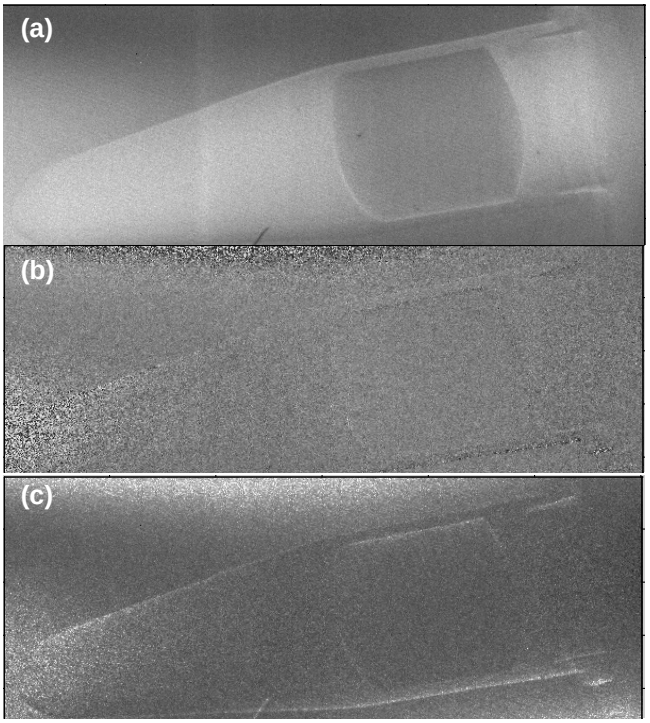

Figure 12. The projection (radiographic) images of the APP-C target in the Aβ-phantom: (a) attenuation contrast, (b) differential phase contrast, and (c) dark field contrast (detector cell: 48 μm).

Conclusion: At the second year milestone of this project, the following summary and discussions are given:

- Overall, the project's progression is on track. The fabrication of the two key components – gratings G1 and G2 – has been successful in the second year, even though it turns out that its success is yet more challenging than anticipated.
- This prototype x-ray phase contrast CT system is working in the PI's Lab at its full functionality as anticipated, although its performance may be further improved by continuous effort in grating fabrication and system optimization.
- With preliminary imaging performance optimization, the prototype x-ray phase contrast CT system have started carrying out the phantom studies specified in the SA #2 of the proposal and is ready for carrying out the specimen studies specified in SA #3.
- With the valued support by this award, the research group led by the PI at Emory University has established an international scientific leadership in x-ray phase contrast CT imaging, demonstrated by its publication in the prestigious scientific journals and conferences, and the invitation by journal's editorial board to review manuscripts, and by federal and non-profit funding agencies for the study sections to review research proposals related to x-ray phase contrast CT imaging. Especially, the PI will be the co-chair of a session entitled "Phase-contrast CT and Few View CT" in the 3rd International

Conference on CT Image Formation in X-ray Computed Tomography (Salt Lake City, Utah, June 22-25, 2014), as well as the chair of another session entitled "Optical, Ultrasound, and Emerging Imaging Techniques" in the AAPM's (American Association of Physicists in Medicine) 52nd Annual Meeting in Austin, TX (August 20-24, 2014).

References:

1. http://www.alz.org/alzheimers_disease_facts_figures.asp, accessed on Dec. 31st, 2010.
2. Roberson ED and Mucke L, "100 years and counting: Prospects for defeating Alzheimer's disease," *Science,* 314:781-84, 2006.
3. Goedert M and Spillantini MG, "A century of Alzheimer's disease," *Science,* v.314, pp 777-81, 2006.Tang X, Ning R, Yu R. and Conover D, "Cone beam volume CT image artifacts caused by defective cells in x-ray flat panel imagers and the artifact removal using a wavelet-analysis-based algorithm" *Med. Phys.,* 28(3): 812-25, 2001.
4. X Wu and H Liu, "Clinical implementation of x-ray phase-contrast imaging: Theoretical foundations and design considerations," *Med. Phys.*, v.30, pp.2169-79, 2003.
5. DM Connor, H Benvenniste, FA Dilmanian, MF Kritzer, LM Miller and Z Zhong, "Computed tomography of amyloid plaques in a mouse model of Alzheimer's disease using diffraction enhanced imaging," *NeuroImage,* v.46, pp 908-14, 2009.
6. F Pfeiffer, T Weitkamp, O Bunk, C David, "Phase retrieval and differential phase-contrast imaging with low-brilliance x-ray sources," *Nature Phys.,* v.2, pp.258-61, 2006.
7. M Bech, TH Jensen, R Feidenhan'l, O Bunk, C David and F Pfeiffer, "Soft-tissue phase-contrast tomography with x-ray tube source," *Phys. Med. Biol.,* v.54, pp.2747-53, 2009.
8. Tang X, Yang Y and Tang S, "Characterization of imaging performance in differential phase contrast CT compared with the conventional CT – Noise power spectrum NPS(k)," *Med. Phys.*, vol. 38, pp. 4386-95, 2011.
9. Tang X, Yang Y and Tang S, "Characterization of imaging performance in differential phase contrast CT compared with the conventional CT – Spectrum of noise equivalent quanta NEQ(k)" *Med. Phys.,* 39(7): 4467-82, 2012.
10. C David, J Bruder, T Rohbeck, C Grunzweig, C Kottler, A Diaz, O Bunk and F Pfeiffer, "Fabrication of diffraction gratings for hard x-ray phase contrast imaging," *Microelect. Eng.,* v.84(5-8), pp1172-77, 2007.
11. Tang X, Ning R, Yu R. and Conover D, "Cone beam volume CT image artifacts caused by defective cells in x-ray flat panel imagers and the artifact removal using a wavelet-analysis-based algorithm" *Med. Phys.,* 28(3): 812-25, 2001
12. Tang X, Hsieh J, Nilsen RA, Hagiwara A, Thibault J and E Drapkin E, "A three-dimensional weighted cone beam filtered backprojection (CB-FBP) algorithm for image reconstruction in volumetric CT under a circular source trajectory," *Phys. Med. Biol.,* v.50, pp.3889-905, 2005.
13. Köhler T and Roessl E, "Noise properties of grating-based x-ray phase contrast computed tomography," *Med. Phys.*, vol. 38, pp. S106-16, (2011).
14. Nickoloff EL, "Measurement of the PSF for a CT scanner: appropriate wire diameter and pixel size," *Phys. Med. Biol.,* v.33, pp.149-55, (1988).
15. Yang Y and Tang X, "The second-order differential phase contrast and its retrieval for imaging with x-ray Talbot interferometry," *Med. Phys., v.39,* pp.7237-53, 2012.